

Multiplicity of infection and the evolution of hybrid incompatibility in segmented viruses

STEVEN A. FRANK

Department of Ecology and Evolutionary Biology, University of California, Irvine, CA 92697-2525 U.S.A.

Some viral genomes are divided into segments. When multiple viruses infect a single cell, progeny form by reassorted mixtures of genomic segments. Hybrid incompatibilities arise when a progeny virus has incompatible segments from different parental viruses. Hybrid incompatibility has been observed in influenza and in the multipartite plant virus *Dianthovirus*. Hybrid incompatibility provides an opportunity to study rates of viral evolution, divergence and speciation, and the extent of epistatic interactions among components of the viral genome. This paper presents mathematical and computer simulation models to study hybrid incompatibility between diverging strains. The models identify multiplicity of infection as a key factor. When many viral particles infect each host cell, the effective ploidy of the genetic system is high. High ploidy dilutes the contribution of each locus to the phenotype, weakening the selective intensity on each locus. Weaker selection on variant alleles allows the population to maintain greater genetic diversity and to be more easily perturbed by stochastic fluctuations. Greater diversity and stochastic fluctuations explore more widely the space of epistatic interactions, causing more frequent shifts among favoured combinations of alleles. Variable ploidy of viral genetics differs from standard Mendelian genetics.

Keywords: epidemiology, epistasis, polyploidy, speciation.

Introduction

Many viral genomes are split into segments. The influenza A and B genomes have eight segments, the large Bunyviridae family of arthropod viruses has three segments. Genomic structures vary widely among other viruses (see reviews in Fields *et al.*, 1996).

The viral capsid releases its individual segments into the host cell upon infection. Each segment replicates in the cell's cytoplasm. The segments act like distinct chromosomes but do not pair and segregate as in Mendelian systems. Instead, new viral particles form by a sampling process that chooses approximately one segment of each type. When multiple viruses infect a single cell, their replicating segments mix. The progeny form by reassorted combinations of genomic segments.

Hybrid incompatibilities arise when a progeny capsid has incompatible segments from different parental viruses. Suppose, for example, that the genome has two segments, *A* and *B*. If two parental viruses, with genotypes A_1B_1 and A_2B_2 , co-infect a cell, then some of the progeny will have hybrid genotypes A_1B_2 or A_2B_1 . A hybrid genotype singly infected into a new cell may

have reduced fitness compared with the two parental types, in which case the progeny suffers from hybrid incompatibility.

Hybrid incompatibility provides a good system for the study of evolutionary problems. One can, for example, analyse rates of viral evolution, divergence and speciation, and the extent of epistatic interactions among components of the viral genome. Sequencing and laboratory studies of segmented viruses will allow one to pinpoint the causes of epistatic interaction at the nucleic acid level. Laboratory evolution and comparative studies of natural populations can test hypotheses about the causes of divergence.

This paper presents mathematical and computer models of the processes that influence hybrid incompatibility between diverging strains. The models identify multiplicity of infection as a key factor. When many viral particles infect each host cell, the effective ploidy of the genetic system is high. Consequently, the selective intensity acting on each mutant is weak because variant alleles tend to have their effects diluted by the other alleles of the same locus present in the host cell.

The models show that weakened selective intensities under high multiplicity of infection allow relatively rapid evolutionary divergence from an ancestral population.

This study measures divergence by the frequency at which populations shift between positively epistatic gene combinations. In particular, 'peak shifts' are analysed between high fitness combinations A_1B_1 , and A_2B_2 , which require crossing the 'valley' of low fitness mixtures A_1B_2 and A_2B_1 . Peak shifts have been studied widely as a model of speciation (Wright, 1940; Barton & Charlesworth, 1984), but those models have not been applied to the unusual genetic structure of segmented viruses.

Background

I found two reports of hybrid incompatibility. In the eight-segmented genome of influenza A, the haemagglutinin protein (segment 4) of the FPV Rostock strain requires cosegregation with the M_2 ion channel protein (segment 7; Grambas & Hay, 1992; Grambas *et al.*, 1992). Haemagglutinin is a crucial surface protein for viral attachment and penetration into host cells. The M_2 protein has various consequences, including pH regulation in cellular regions where haemagglutinin is active. FPV Rostock haemagglutinin requires its cosegregating M_2 variant to influence pH in particular ways during infection. FPV Rostock haemagglutinin with heterologous M_2 from the Weybridge strain fails during infection (reviewed in Lamb & Krug, 1996).

The second case of hybrid incompatibility occurs in multiparticle genomes. In these viruses, the individual segments are packaged into distinct capsids, each capsid containing only one of the genomic segments (Matthews, 1991). Successful infection requires co-infection by at least one capsid of each segment type. In this peculiar system, full viral genomes occur only within host cells. Reassortment follows when segments infecting a target cell come from different parental host cells. In the two-segment genome of red clover necrotic mosaic *Dianthovirus*, two strains have been identified such that segment 1 from the first strain combined with segment 2 from the second strain creates a successful infection, whereas the reciprocal combination exhibits hybrid incompatibility (Rao & Hiruki, 1987).

Model

This section begins with the main assumption and a preliminary analysis. The mathematical analysis is followed by a computer simulation to measure the average waiting time between peak shifts. The mathematical analysis provides a qualitative guide to the forces involved. Those qualitative insights aid interpretation of the quantitative output from the computer simulations.

Fitness

Each virus carries two segments, A and B . Segment A has two genetic variants, A_1 and A_2 , and segment B has two variants, B_1 and B_2 . The number of progeny viruses produced by an infected cell depends on the genotypes of the viruses in that cell. If a cell has a single virus of genotype A_1B_1 or A_2B_2 , the cell produces k viral progeny. If a cell has either hybrid genotype, A_1B_2 , or A_2B_1 , the cell produces $k(1-s)$ progeny, where the fitness penalty for hybrids is s . For convenience, the following analysis drops the k and uses 1 or $1-s$ for fitness.

When multiple viruses infect a cell, let p be the frequency of the A_1 variant among the A segments within the cell, and let q be the frequency of the B_1 variant among the B segments within the cell. Variants within a cell can interact in two ways to determine the number of viral progeny (fitness) from that cell. The additive model sums the probabilities of conforming interactions (A_1B_1 and A_2B_2) and hybrid interactions (A_1B_2 and A_2B_1), each type of interaction weighted by its fitness. Thus, the total fitness of viruses within a cell is

$$\begin{aligned} w &= pq + (1-p)(1-q) \\ &\quad + (1-s)[p(1-q) + q(1-p)] \\ &= 1 - s(p + q - 2pq). \end{aligned} \quad (1)$$

Average fitness is

$$\bar{w} = 1 - s(\bar{p} + \bar{q} - 2\bar{p}\bar{q}) \quad (2)$$

where \bar{p} and \bar{q} are the average frequencies in the population for A_1 and B_1 , respectively, and $\bar{p}\bar{q} = \text{Cov}(p, q) + \bar{p}\bar{q}$. If we let $\bar{p} = \bar{q}$, then the total fitness penalty for hybrid interactions is

$$\begin{aligned} S &= s[\bar{p} + \bar{q} - 2\bar{p}\bar{q} - 2\text{Cov}(p, q)] \\ &= 2s[\bar{p} - \bar{p}^2 - \text{Cov}(p, q)] \\ &= 2s\bar{p}(1 - \bar{p}) \left[1 - \frac{\text{Cov}(p, q)}{\bar{p}(1 - \bar{p})} \right] \\ &= 2s\bar{p}(1 - \bar{p}) \left[1 - \frac{\text{Corr}(p, q)}{\bar{m}_h} \right] \end{aligned} \quad (3)$$

where $\text{Corr}(p, q)$ is the correlation between p and q within hosts, and $\bar{p}(1 - \bar{p})/\bar{m}_h = \text{Var}(p)$, where \bar{m}_h is the harmonic mean multiplicity of infection, m , for the number of viruses infecting a host cell. The analysis here assumes that there is no genetic correlation between viruses within a host cell.

As $\text{Corr}(p, q)$ rises, an increasing proportion of alleles occurs in complementary mixtures, that is, A_1B_1 and A_2B_2 combinations. Selection acts only against hybrid combinations, so an increase in complementary mixtures

reduces the total fitness penalty. As \bar{m}_h rises, cells are infected by more viruses, increasing the frequency of hybrid interactions and raising the total fitness penalty.

The above discussion applies to an additive model of fitness. Alternatively, in a complementation model of fitness interactions, full fitness occurs when there is at least one conforming pair (A_1B_1 , or A_2B_2), otherwise the cell has the hybrid fitness.

Thus,

$$w = \begin{cases} 1 - s & p = 1, q = 0 \\ 1 - s & p = 0, q = 1 \\ 1 & \text{otherwise.} \end{cases} \quad (4)$$

Force of selection on gene frequency change in the additive model

The population states $\bar{p} = \bar{q} = 0$ and $\bar{p} = \bar{q} = 1$ are attracting equilibria (peaks). Natural selection opposes a shift from one peak to the other because the intermediate hybrids have lower fitness. Peak shifts occur only when stochastic sampling processes perturb gene frequencies sufficiently to favour a transition from one equilibrium to the other. As the force of natural selection weakens, the probability of a transition increases.

One can measure the force of selection by the rate of gene frequency change in the absence of stochastic factors. Price's (1970) equation provides a convenient way to write the rate of gene frequency change (Frank, 1995). The Price equation for $\Delta\bar{p}$, the change per generation in the population frequency of A_1 , is

$$\bar{w}\Delta\bar{p} = \text{Cov}(w, p) + E(w\Delta p).$$

In this model, the change in gene frequency between the viruses that infect the cell and the viruses produced by the cell is zero. Thus, $\Delta p = 0$ and we can drop the second term on the right side. Expanding $\text{Cov}(w, p)$ yields

$$\begin{aligned} \bar{w}\Delta\bar{p} &= \text{Cov}(1 - s(p + q - 2pq), p) \\ &= -s[\text{Var}(p) + \text{Cov}(p, q) - 2\text{Cov}(pq, p)]. \end{aligned} \quad (5)$$

If we write the variables p and q as deviations from their population means, $p = \bar{p} + \delta p$ and $q = \bar{q} + \delta q$, then

$$\begin{aligned} \text{Cov}(pq, p) &= \text{Cov}((\bar{p} + \delta p)(\bar{q} + \delta q), p) \\ &= \bar{q}\text{Var}(p) + \bar{p}\text{Cov}(q, p) + \text{Cov}(\delta p\delta q, \delta p) \end{aligned}$$

Substituting this into eqn 5 yields

$$\begin{aligned} \bar{w}\Delta\bar{p} &= 2s\text{Var}(p)[(\bar{q} - 1/2) \\ &\quad + \beta_{q,p}(\bar{p} - 1/2) + \beta_{\delta p\delta q, \delta p}], \end{aligned} \quad (6)$$

where the regression of q on p , $\beta_{q,p}$, measures the association between p and q within host cells, and the regression of $\delta p\delta q$ on δp , $\beta_{\delta p\delta q, \delta p}$, measures the tendency for gene frequencies of A_1 and B_1 within a host cell to be complementary as the deviation of p from its population average increases within a cell. Although the two regression terms can influence the dynamics (see below), the net force of selection, $\Delta\bar{p}$, will typically be dominated by $\text{Var}(p)$ when measured for given values of \bar{p} , \bar{q} and s .

$\text{Var}(p) = \bar{p}(1 - \bar{p})/\bar{m}_h$ where \bar{m}_h is the harmonic mean of the multiplicity of infection, m . As the harmonic mean of m increases, the variance in fitness among cells declines, and the force of selection opposing stochastic peak shifts also declines.

Stochastic fluctuations: effective population size and multiplicity of infection

This section turns to the stochastic fluctuations that cause peak shifts against the opposition of the deterministic force of selection. The stochastic fluctuations depend on the effective population size, N_e . The various parameters that control population size and sampling also provide an introduction to the key parameters of the stochastic computer model presented in a later section.

The population consists of C host cells, each host cell infected by m viruses (multiplicity of infection). The total population of viruses is $N = C\bar{m}$, where overbars denote averages. Rounding error is ignored when converting between integer values and continuous values.

Some of the following analyses hold m constant among host cells. In other cases, m varies among cells according to a Poisson process in which host cells with no viruses, $m = 0$, are ignored. In this truncated Poisson process, the probability of $m \geq 1$ viruses in a particular cell is

$$f(m) = \lambda^m e^{-\lambda} / [m!(1 - e^{-\lambda})] \quad (7)$$

where λ would be the average value of m if cells with zero viruses were included. However, this analysis ignores cells with zero viruses. The average number of viruses in cells with at least one virus is $\bar{m} = \lambda/(1 - e^{-\lambda})$. Thus, given a value for \bar{m} , we can solve for the λ -value needed to calculate the various probabilities $f(m)$.

The effective population size is the reciprocal of the probability of randomly choosing the same allele twice from a population. Specifically, if we choose with replacement two viral alleles from the population at random, in proportion to each allele's probability of being transmitted to the next generation, the reciprocal of the probability of choosing the same allele twice is N_e . Thus, N_e is the effective number of nonduplicated members of a population, a measure of sample size.

The smaller the sample size, the greater the tendency for stochastic fluctuations.

Standard calculations show that $N_e = C\bar{m}_h$, the number of host cells multiplied by the harmonic mean of the multiplicity of infection. When m does not vary among cells, then $\bar{m}_h = \bar{m}$ and $N_e = N$.

As N_e declines, stochastic fluctuations increase and the average waiting time until the next peak shift decreases (Wright, 1940; Barton & Charlesworth, 1984).

Opposition between deterministic selection and stochastic perturbation

The analysis has thus far contrasted two opposing forces that influence the average time between peak shifts, a measure of the rate of evolutionary divergence between separated populations. First, higher multiplicity of infection raises the ploidy, partially masks deleterious variants, and reduces the deterministic force by which natural selection removes those deleterious variants. Weaker deterministic selection makes it easier for a population to cross a low-fitness valley between two peaks.

Second, lower effective population size increases stochastic fluctuations and reduces the waiting time before a perturbation pushes the population across a fitness valley to the opposite peak.

The effective population size and the harmonic mean of multiplicity of infection may be confounded because effective population size is $N_e = C\bar{m}_h$. However, by controlling the number of infected host cells, C , one can vary N_e and \bar{m}_h independently and show their separate effects. This is presented below in the computer analysis.

Strong association of complementary alleles at low multiplicity of infection

A third force arises from associations between complementary variants, A_1B_1 or A_2B_2 . Equations 5 and 6 show the effects of associations in the covariance and regression terms. Those terms measure the association between the p and q within hosts, that is, the association between the frequencies of A_1 and B_1 within hosts. The analytical expressions do not provide simple forms for these associations because of the frequency-dependent nature of selection in this problem. However, qualitative aspects can be described as follows.

Increases in complementary associations reduce the deterministic force of selection. Consider, for example, the case in which the number of viruses infecting each cell is one. If each virus has a complementary genotype A_1B_1 or A_2B_2 , no selection occurs. Thus, a positive association between A and B variants within viruses

reduces selection and increases the frequency of peak shifts.

Multiplicity of infection, m , has the strongest effect on the strength of complementary associations between A and B variants within host cells. In this model, different viruses infecting the same cell are genetically uncorrelated, so all associations between p and q arise from correlations (linkage disequilibrium) between A_1 , and B_1 , within individual viruses. Random sampling of viruses reduces the total association within cells by $1/m$. Multiple infection also provides opportunity for reassortment of segments during the production of new viruses. Reassortment reduces the correlation between A and B alleles within viruses. Thus, the association within host cells can be high when $\bar{m}_h \rightarrow 1$, but declines quickly as \bar{m}_h rises.

Stronger selection, s , raises the association between p and q by disfavouring hybrid mixtures. Higher N_e increases the association by reducing stochastic fluctuations and raising the relative contribution of the deterministic selection that creates associations. Increased mutation provides more variation for selection to create associations, but mutation breaks down existing associations by altering allelic state.

In summary, low \bar{m}_h promotes complementary associations between A and B alleles, reducing the force of deterministic selection and decreasing the average waiting time between peak shifts. Associations decay rapidly as \bar{m}_h rises above one. Thus, the contribution of allelic associations occurs mostly when multiplicity of infection is low.

Average waiting time between peak shifts

The model has four key parameters: the strength of selection, s , the effective population size, N_e , the mutation rate, μ , and the multiplicity of infection, \bar{m}_h . This section presents a computer simulation to show how these four parameters influence the average waiting time between peak shifts.

Each run begins with $C = N_e/\bar{m}_h$ host cells and $N = C\bar{m}$ viruses. Initially, all alleles are A_1 and B_1 , thus $\bar{p} = \bar{q} = 1$. Viruses are assigned randomly to host cells. In some runs, all cells receive a constant number $m = \bar{m}$ viruses. In other runs, the distribution of viruses per cell follows the truncated Poisson distribution with average multiplicity of infection \bar{m} .

The relative fitness of viruses from each host cell is calculated by eqn 1 for the additive model or eqn 4 for the complementation model. N progeny viruses are created by sampling host cells with replacement in proportion to fitness. A host cell produces a progeny virus by random sampling with replacement of one A

segment and one *B* segment. The allele at each segment mutates to the opposite allelic state with probability μ .

The initial population is at the A_1B_1 peak. A peak shift occurs when at least 70% of the viral population consists of the A_2B_2 genotype, and a shift back when at least 70% of the viral population consists of the A_1B_1 genotype. Each run continues for 10^7 generations or 100 peak shifts, whichever comes first. After stopping, the average waiting time for a peak shift is calculated as the number of generations divided by the number of peak shifts.

Figure 1 shows results from a factorial design with $4 \times 3^3 = 108$ parameter combinations (see figure legend). In this design, the multiplicity of infection per cell is constant at $\bar{m}_h = \bar{m}$. For $\bar{m} \geq 2$, the average waiting time

decreases strongly with a rise in multiplicity of infection. Stronger selection, s , increases the waiting time by imposing a stronger barrier to cross the fitness valley between peaks. Higher mutation rates and lower effective population sizes reduce the time between shifts by enhancing the stochastic perturbations to the population.

For many parameters, $\bar{m}_h = 1$ causes a lower time between peak shifts than $\bar{m}_h = 2$. As $\bar{m}_h \rightarrow 1$, the statistical association increases between complementary *A* and *B* alleles, reducing the strength of deterministic selection and raising the relative contribution of stochastic perturbations.

Figure 2 shows a more detailed picture of waiting times for low \bar{m}_h . In this analysis, the number of viruses

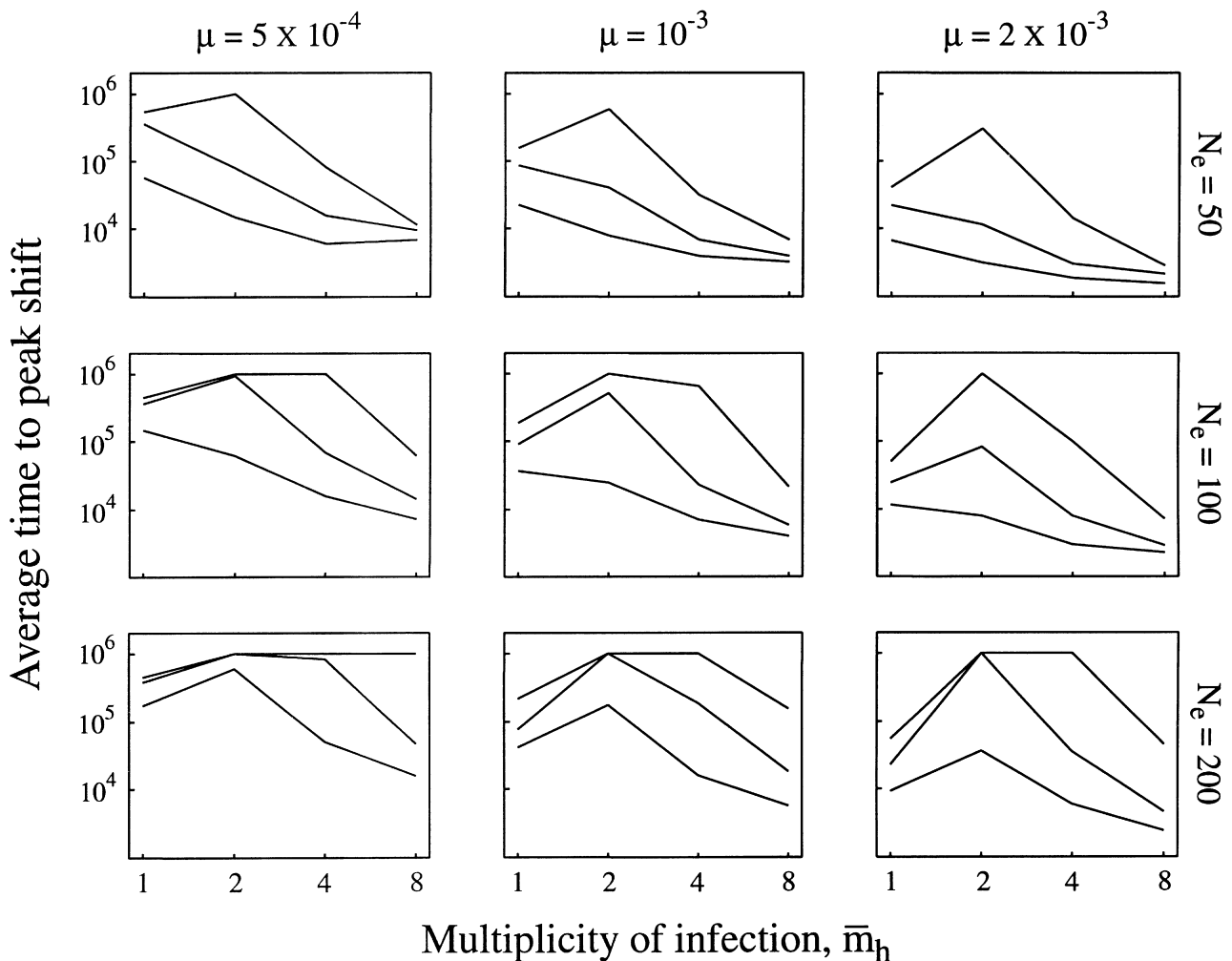


Fig. 1 Average waiting time between peak shifts. Values from the computer simulations occur at 108 parameter combinations over the following levels: constant multiplicity of infection per cell $\bar{m}_h = \bar{m} = 1, 2, 4, 8$; selective coefficient $s = 0.05, 0.1, 0.2$ (lines in each panel, the lower lines have lower s -values); mutation rate $\mu = 5 \times 10^{-4}, 10^{-3}, 2 \times 10^{-3}$; and effective population size, $N_e = 50, 100, 200$. These runs used the additive fitness model.

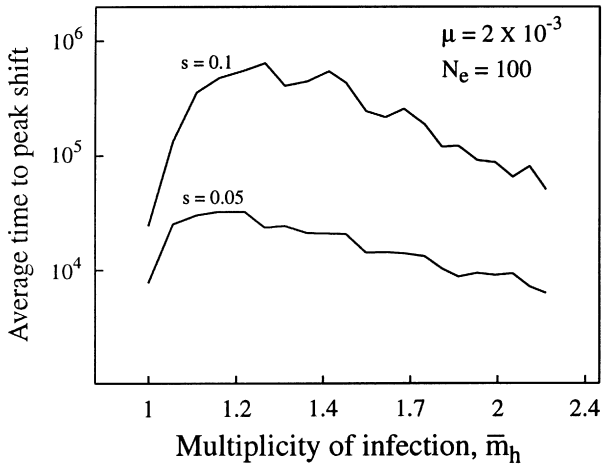


Fig. 2 Average waiting time between peak shifts for low harmonic mean multiplicity of infection. The abscissa is scaled logarithmically.

per cell varied according to the truncated Poisson distribution. The waiting times rise as \bar{m}_h rises above one because multiple infections reduce associations within host cells and provide an opportunity for reassortment of segments. As \bar{m}_h continues to rise, the tendency of higher multiplicity of infection to reduce waiting times outweighs further decreases in statistical associations between *A* and *B* alleles.

Figure 3 shows the same parameter combinations as Fig. 1, but with the complementation fitness scheme of eqn 4 rather than the additive fitness scheme used throughout the analysis. The complementation fitness scheme has lower waiting times between peak shifts. This occurs because complementation produces full fitness in cells with at least one complementary pair of *A* and *B* alleles. This protection of hybrid combinations greatly reduces the force of deterministic selection at high multiplicity of infection, increasing the role of

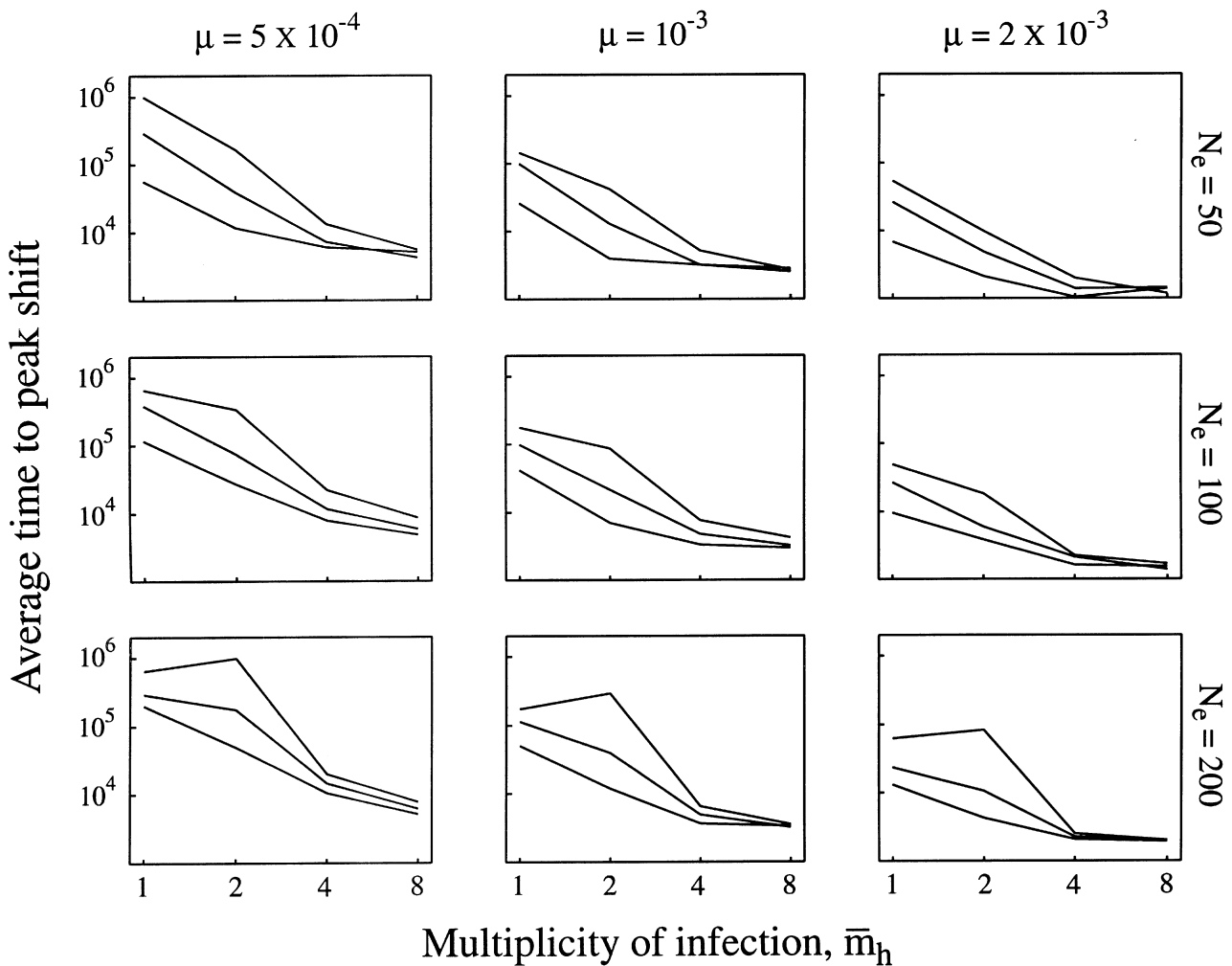


Fig. 3 Average waiting time between peak shifts for the complementation fitness model. All parameter values the same as in Fig. 1.

stochastic perturbations that shift the population from one peak to the other.

General aspects of the peak-shift model

The computer model used relatively high mutation rates and small effective population sizes. This was necessary to obtain sufficient numbers of peak shifts within a reasonable time. Lower mutation rates and higher population sizes will increase the average waiting times for peak shifts.

The model assumed only a single epistatic combination with one locus on each of two segments. There are likely to be many such epistatic combinations, so the waiting time for one peak shift will be reduced by the simultaneous fluctuations of the many different combinations.

The model followed from the biology of segmented viruses. But the assumptions may apply to other group-structured organisms. The model assumes only that genetic interactions among group members cause all group members to have the same individual fitness. This may occur, for example, when the genotypes of group members interact to determine the level of environmental toxicity or other environmental factors that affect all group members (Wilson, 1980; Wade & Goodnight, 1998; Wolf *et al.*, 1999).

Consequences for viral evolution

High multiplicity of infection weakens the selective intensity per segment. The multiplicity of infection is, in effect, the ploidy level for a genome during its period of expression. High ploidy dilutes the contribution of each locus to the phenotype, weakening the selective intensity on each locus. Weaker selection on variant alleles allows the population to maintain greater genetic diversity and to be more easily perturbed by stochastic fluctuations. Greater diversity and stochastic fluctuations explore more widely the space of epistatic interactions, causing more frequent shifts among favoured combinations of alleles. Variable ploidy of viral genetics differs from standard Mendelian genetics.

Rapid evolution during periods of high multiplicity of infection may generate new viral strains. Culturing techniques within laboratory strains may enhance the rate of evolutionary change as the multiplicity of infection increases. Such change in cultured stocks may lead to evolutionary divergence from the ancestral strain.

High multiplicity of infection often leads to competition between co-infecting viruses within a cell (Holland, 1990). The analyses in this paper prevented competition within cells to focus the study on rates of evolutionary divergence. A separate study analysed the

dynamics of within-cell competition (Frank, 2000; see also Szathmáry, 1993; Kirkwood and Bangham, 1994).

The model suggests that increased multiplicity of infection raises the rate of evolutionary divergence between separated populations. This leads to two testable predictions. First, infections with higher viral densities within hosts will diverge more quickly from an ancestral population than will infections with lower viral densities within hosts. Second, laboratory studies that manipulate multiplicity of infection can test in a controlled setting the rates of evolutionary divergence among strains. The model suggests that higher multiplicity of infection will lead to greater hybrid incompatibility between diverging populations.

Acknowledgements

National Science Foundation grant DEB-9627259 supports my research. I thank R. M. Bush for helpful comments.

References

- BARTON, N. H. AND CHARLESWORTH, B. 1984. Genetic revolutions, founder effects, and speciation. *Ann. Rev. Ecol. Syst.*, **15**, 133–164.
- FIELDS, B. N., KNIPE, D. M. AND HOWLEY, P. M. 1996. *Fundamental Virology*, 3rd edn. Lippincott–Raven, Philadelphia.
- FRANK, S. A. 1995. George Price's contributions to evolutionary genetics. *J. Theor. Biol.*, **175**, 373–388.
- FRANK, S. A. 2000. Within-host spatial dynamics of viruses and defective interfering particles. *J. Theor. Biol.*, **206**, 279–290.
- GRAMBAS, S., BENNETT, M. S. AND HAY, A. J. 1992. Influence of amantadine resistance mutations on the pH regulatory function of the M_2 protein of influenza A viruses. *Virology*, **191**, 541–549.
- GRAMBAS, S. AND HAY, A. J. 1992. Maturation of influenza A virus haemagglutinin—estimates of the pH encountered during transport and its regulation by the M_2 protein. *Virology*, **190**, 11–18.
- HOLLAND, J. J. 1990. Defective viral genomes. In: Fields, B. N. (ed.) *Virology*, 2nd edn, pp. 151–165. Raven Press, New York.
- KIRKWOOD, T. B. L. AND BANGHAM, C. R. M. 1994. Cycles, chaos, and evolution in virus cultures: a model of defective interfering particles. *Proc. Nat. Acad. Sci. U.S.A.*, **91**, 8685–8689.
- LAMB, R. A. AND KRUG, R. M. 1996. Orthomyxoviridae: the viruses and their replication. In: Fields, B. N., Knipe, D. M. and Howley, P. M. (eds) *Fundamental Virology*, 3rd edn, pp. 605–647. Lippincott–Raven, Philadelphia.
- MATTHEWS, R. E. F. 1991. *Plant Virology*, 3rd edn. Academic Press, New York.
- PRICE, G. R. 1970. Selection and covariance. *Nature*, **227**, 520–521.
- RAO, A. L. N. AND HIRUKI, C. 1987. Unilateral compatibility of genome segments from two distinct strains of red clover necrotic mosaic virus. *J. Gen. Virol.*, **68**, 191–194.

- SZATHMÁRY, E. 1993. Co-operation and defection: playing the field in virus dynamics. *J. Theor. Biol.*, **165**, 341–356.
- WADE, M. J. AND GOODNIGHT, C. J. 1998. Perspective: The theories of Fisher and Wright in the context of metapopulations: When nature does many small experiments. *Evolution*, **52**, 1537–1553.
- WILSON, D. S. 1980. *The Natural Selection of Populations and Communities*. Benjamin/Cummings, Menlo Park, CA.
- WOLF, J. B., BRODIE, E. D. AND MOORE, A. J. 1999. Interacting phenotypes and the evolutionary process. II. Selection resulting from social interactions. *Am. Nat.*, **153**, 254–266.
- WRIGHT, S. 1940. Breeding structure of populations in relation to speciation. *Am. Nat.*, **74**, 232–248.